

Defects, Vortices, and Critical Current in Josephson-Junction Arrays

W. Xia and P. L. Leath

Physics Department, Rutgers University, Piscataway, New Jersey 08855-0849

(Received 5 July 1989)

The breakdown phenomena of a resistively shunted two-dimensional Josephson-junction array with a single defect driven by an external current at zero temperature are studied numerically. The nonlinear Josephson relation causes the formation of vortices at the tips of the defect at i_v and thus lowers the current enhancement there. Above a higher critical current i_c the vortices depin from the defect and march across the sample producing a voltage. The critical current i_c is studied versus defect size. Various dynamical properties and the I - V characteristics of the array are explained in the context of vortex motion. From the observed features the critical behavior of a randomly disordered array is predicted.

PACS numbers: 74.60.Jg, 05.60.+w, 74.70.Mq

Breakdown phenomena in various inhomogeneous systems have been studied extensively over the past four years.¹⁻³ The effects of the most critical defects turn out to be very important in understanding the breakdown process. Recently, Leath and Tang⁴ have studied the critical current in an inhomogeneous superconducting system by looking into the current distributions in both the normal and superconducting regions utilizing the linearized Ginzburg-Landau equations. These linearized equations and the boundary conditions turn out to be similar to those of the random-resistor network problem. While the linearized problem is easier to analyze, the nonlinear effects turn out to be essential in accounting for the appearance of vortices (topological excitations) and their dissipation and therefore the breakdown of the superconducting weak-link system. In this Letter we report results of studying the breakdown process in superconducting weak-link systems with a simple defect by using resistively shunted Josephson-junction arrays. We study numerically the role of a single critical defect of varying size in the resistively shunted junction array and the dynamical properties of the vortices caused by the defect in the system, and use this to predict the behavior of randomly disordered arrays. The presence of the defect causes drastically different behavior from that previously reported by authors of numerical^{5,6} and experimental⁷ studies of perfect arrays.

The system we studied is one in which superconducting grains are uniformly distributed in two dimensions to form the sites of a square lattice. Within our approximation each grain (site) is described by a complex superconducting order parameter $\Delta = \Delta_0 e^{i\varphi}$, where Δ_0 is constant for all grains and φ varies from grain to grain. Each grain is coupled to its nearest-neighboring grains by the resistively shunted junctions (bonds). Figure 1(a) shows a small 4×5 array. Each junction, as illustrated in Fig. 1(b), consists of a resistor and a microbridge in parallel. Here the charging effect, which is responsible for the hysteresis of the junctions, has been neglected; this approximation is valid for proximity-effect junctions.⁸ The current-conservation rule for a single junction

gives

$$I_0 \sin(\varphi_1 - \varphi_2) + \frac{h}{2eR} \left(\frac{d\varphi_1}{dt} - \frac{d\varphi_2}{dt} \right) = I_{12}, \quad (1)$$

where I_0 is the maximum supercurrent that can flow in the junction between grains 1 and 2 and φ_1 and φ_2 are the phases of the respective grains; R and I_{12} are the normal resistance and total current flowing between the two grains. On the left-hand side of Eq. (1), the first term is the well-known Josephson current⁹ and the second term is the normal current due to the voltage caused by the changing phases between grains. After defining $\tau = 2eRI_0 t / h$ and $i_k^{\text{ext}} = I^{\text{ext}} / I_0$, the dimensionless phase equation of the k th grain of an array with identical junctions is given by

$$\sum_l \left(\frac{d\varphi_k}{d\tau} - \frac{d\varphi_l}{d\tau} \right) = i_k^{\text{ext}} - \sum_l \sin(\varphi_k - \varphi_l), \quad (2)$$

which can be written in the generalized matrix form

$$\mathbf{G} \frac{d\varphi}{d\tau} = \mathbf{C}(\varphi), \quad (3)$$

where the summation is over nearest-neighbor sites and i_k^{ext} is the normalized externally applied current at site k . External currents are only supplied or withdrawn from the top and bottom rows. The set of equations (2) or (3)

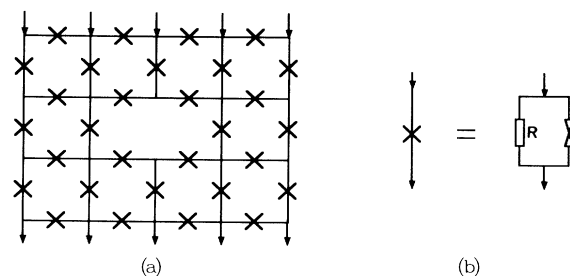


FIG. 1. (a) A 5×4 junction array with a single defect (single missing junction). (b) Each resistively shunted junction consists of a microbridge and a resistor in parallel.

for each site is then solved by multiplying Eq. (3) by the matrix integration factor G^{-1} and integrating numerically by using a fourth-order Runge-Kutta integration scheme with appropriate initial phases $\varphi_i(0)$. This technique which was used by Chung, Lee, and Stroud⁵ is equivalent to that used by Shenoy and by Mon and Teitel⁶ for perfect arrays.

In the case of a perfect array of identical junctions with uniform initial conditions for Eq. (2), the array behaves like a giant single junction.¹⁰ That is, for the external current i less than $i_c = 1$, there is no voltage across the sample; for i greater than i_c the phase difference across any junction behaves like a staircase of steps versus time with a regular period¹¹ between steps,

$$T = \frac{h\pi}{eR} (i^2 - i_c^2)^{-1/2}. \quad (4)$$

The time-averaged voltage over several periods is given by¹¹ $V = NR(i^2 - i_c^2)^{1/2}$, where N is the number of junctions in the vertical direction. As the external current becomes very large the I - V curve shows the Ohmic behavior of an array of normal resistors.

The situation is substantially different when there are defects present. To study this effect we introduce a horizontal defect or slit by taking one or several adjacent vertical junctions out of the center of the uniform array [Fig. 1(a)]. The current thus has to flow around the defect and therefore the current density near the defect tip is enhanced. When the external current is below the critical current of the sample the phases of the grains are constant in time although inhomogeneous in space and all the currents are in the form of supercurrents and thus there is no voltage across the sample. When the current is small the supercurrent distribution is approximated by a dipole distribution as in the linearized problems. Because of the current enhancement at the tip of the defect, the junction closest to the defect will reach its maximum current $i_0 = 1.0$ first. We define i_v to be the applied current for which the supercurrent in the most critical junction(s) (i.e., those carrying the most supercurrent, which in this case are those at each end of the defect) reaches $i_0 = 1.0$. As the external current is increased above i_v we find that the system does not show any dissipation but rather the current is redistributed by the formation of a vortex (or antivortex) attached to each end of the defect. The formation of vortices at each end of the defect is the result of the coherence and nonlinearity present in this model. This feature was absent in the previous model studied by Leath and Tang⁴ and others.¹⁻³ The physical consequence of the vortex formation is that the vortex current tends to cancel the supercurrent in the junction closest to the defect and to add to the current in the junctions further out. This makes the current distribution near the defect more flat as current is shared with the further neighbors. In Fig. 2 we show the supercurrent distribution, versus position away from the defect tip along the axis of the defect, both below

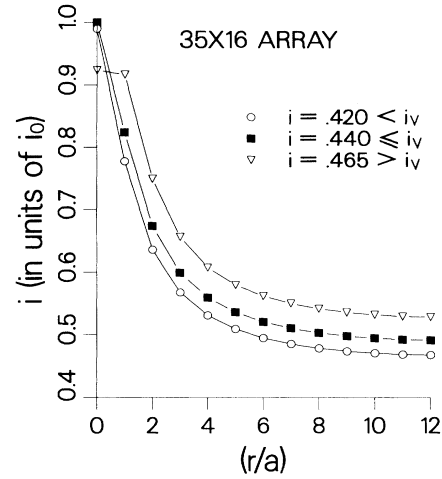


FIG. 2. The supercurrent i/i_0 in the vertical junctions in the central row vs distance r from the tip of the defect.

and above i_v for a 35×16 junction array with defect length $A = 10a$, where a is the lattice spacing.

Once the pinned vortices are formed at the tips of the defect they will experience a Lorentz force $F_L \propto J\varphi_0/c$, perpendicular to the external current, where φ_0 is the vortex quantum which is 2π in this case and J is the external current density at the center of the vortices.¹² When the external current reaches i_c the Lorentz force on the vortex equals the pinning force and the vortex breaks free and starts to move under the influence of the Lorentz force and thus through $d\varphi/d\tau$ to produce a voltage across the sample. Therefore i_c is the critical current at which a voltage first appears. Of course the vortex and antivortex move away from each other in the directions perpendicular to the transport current. In Fig. 3 we plot the magnitudes of the horizontal component of the supercurrent versus lattice position at different times for junction arrays with periodic boundary conditions in the horizontal direction. The length of the defect is $10a$; the width is a (one lattice spacing). Figures 3(a)–3(e) are snapshots of a 35×34 array at different times (in units of τ) with external current $i = 0.50 > i_c = 0.472$. One can see clearly the periodic creation and motion of the vortices (because of the horizontal periodic boundary conditions the vortex and antivortex actually annihilate each other at the boundaries). In the present problem the external current is kept steady and therefore there are constant creation and depinning of the moving vortices with a period T which determines the spacing between moving vortices. The rate of phase change, $d\varphi/d\tau$, monitored here at a site in the top row of the array, oscillates periodically corresponding to the periodic motion of the vortices in the central row. Since the voltage is, by definition, proportional to the time average of the phase change over a period, it is inversely proportional to the period T . We find that period $T = T_A(i^2 - i_c^2)^{-1/2}$, similarly to Eq. (4), for i above and sufficiently close to

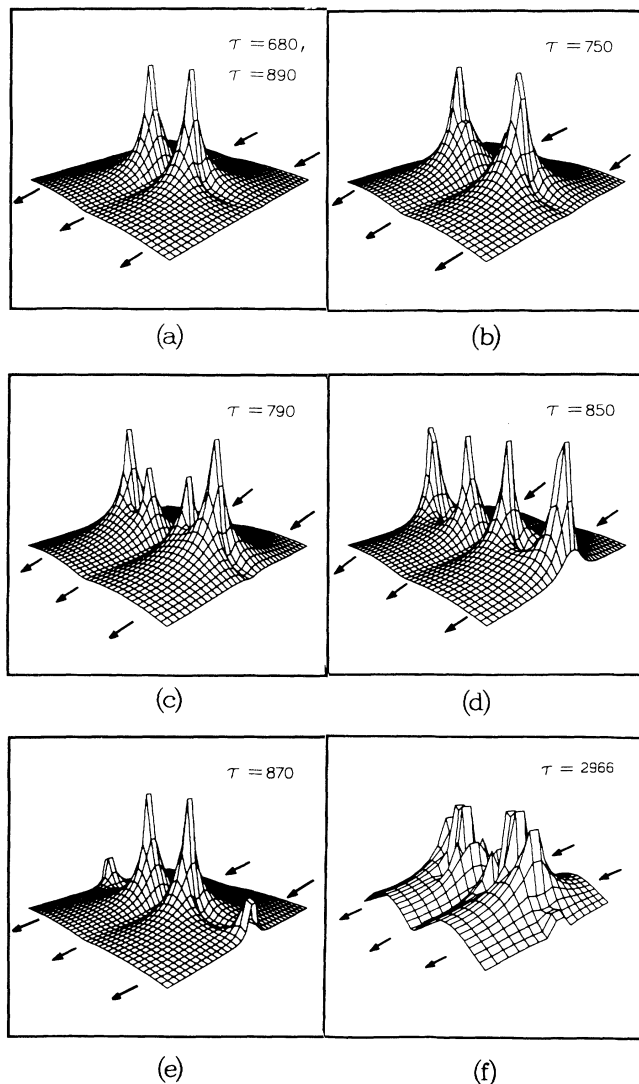


FIG. 3. (a)–(e) Snapshots of vortex movement in a 35×34 array at $i > i_c$ at different times indicated by τ . After (e) the picture returns to (a) and repeats the (a)–(e) process indefinitely. (f) A snapshot at $i > i_{c3}$ when vortices appear in the adjacent rows immediately below and above the central row in a 35×16 array. A series of snapshots here would have shown the horizontal movement of these vortices as well.

i_c , and T_A depends on the size of the defect. As indicated from the numerical simulation, when the current is above and close to the critical current i_c the core of the vortex is just one lattice plaquette and thus the moving vortices produce a voltage drop over each junction in the central row. In Fig. 4(a) we plot the logarithm of the critical current i_c versus the logarithm of the defect size A for different system sizes. A straight line with slope of $-\frac{1}{2}$ is also drawn. The physical origin of the straight line will be discussed in the next paragraph. One can see that the data points approach the straight line as the

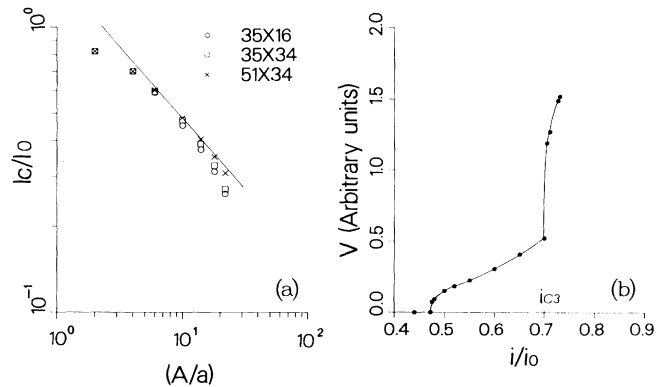


FIG. 4. (a) Critical current i_c/i_0 plotted vs defect size A/a on a logarithmic scale. (b) I - V curve of a junction array with a single defect of length $10a$ (nine missing junctions).

sample size becomes larger and larger. The deviation seems to be due to the boundaries of the sample. This behavior is important for predicting the critical behavior of disordered arrays.

To obtain the scaling relation between i_c and A [the straight line in Fig. 4(a)] one must first estimate the pinning force on the vortex due to the defect and the antivortex at the other end. The interaction between vortex and antivortex will be small, when compared with the defect pinning energy if the defect is sufficiently long, and normally can be neglected. Although it is extremely difficult to calculate the pinning force for a vortex outside a rectangular defect, it is reasonable to assume that the pinning force is more or less a constant when the length of a long thin defect is changed while the geometry at the end of the defect, near which the vortex is bound, is kept the same. The current enhancement at the tip of the defect, however, is very sensitive to the change of the defect length because the external current must flow around the defect. For a long defect i_c tends to zero and the Poisson equation can be used to estimate the current enhancement at the defect tip. The current at the tip is given by $i_{\text{tip}} = i_\infty [1 + (A/2d)^{1/2}]$ for $A \gg d$, where i_∞ is the external current at the boundary. Using the fact that at i_c the Lorentz force equals the pinning force which is approximately a constant, we have

$$i_c = i_\infty = \text{const}/[1 + (A/2d)^{1/2}] \sim A^{-1/2} \quad (5)$$

for $A \gg d$. This scaling relation is the same as that of the random-resistor problem.^{2,3}

When the external current is increased further we observed that the adjacent rows of junctions immediately below and above the central row develop voltages and as a result the I - V curve jumps abruptly at i_{c3} [see Fig. 4(b)]. This abrupt jump in the I - V curve is simply due to the creation and motion of additional vortices in the adjacent rows. These additional vortices are seen, in Fig. 3(f), near the ends of the defect at $i = 0.7065 > i_{c3}$

≈ 0.7045 on a 35×16 array. The junctions in the central row near the defect carried the most current and hence the central row was the first to develop voltages (or break down). The next most critical junctions lie immediately above and below in the adjacent rows and hence the creation of additional vortices here cause these rows to break down next. So at current i_{c3} the vortices in the adjacent rows begin to move and produce additional voltages in the sample. In the cases where the vortices are formed and depinned at different frequencies in the three rows, we find that $d\phi/d\tau$, monitored at the top of the system, will have a different and complicated oscillating pattern at each different external current i . At i very close to i_{c3} , $d\phi/d\tau$ will have an oscillating pattern which switches intermittently in time; i.e., a plot of $d\phi/d\tau$ shows a train of periodic oscillations which is disrupted by chaotic-appearing intervals. Such oscillating patterns occur because the periodic oscillations due to the vortex motion in the central row are superimposed with the oscillations of the vortex motion in the adjacent rows. The fact that the burst appears to be chaotic instead of periodic is due to the interaction between the vortices in different rows. As the external current i is increased further the periods of the vortex motion in the adjacent rows become shorter. The oscillating patterns at larger values of current i are periodic if T_1/T_2 is a simple rational number, quasiperiodic if T_1/T_2 is close to a simple rational number, and chaotic otherwise. T_1 and T_2 are the periods of vortex motion in the central and adjacent rows, respectively. Presumably there are similar and smaller jumps in the I - V curve as additional rows produce vortices and voltage drops but we could not resolve these features although we did observe at higher currents that additional rows develop voltages before the whole system breaks down.

From previous studies¹⁻⁴ it is known that the critical behavior of an array with random defects is determined by the distribution and behavior of the most critical defects. The behavior of the most critical defects can be determined by studying them one at a time as we have done here. Because the scaling relation between the critical current and defect size in the present problem is like that of the linearized problems for a single defect, it is clear that the breakdown current I_1 of real randomly disordered superconducting arrays will vanish logarithmically versus system size L , and it is given by²

$$I_1/L \propto 1/[1 + K(\ln L)^\alpha], \quad (6)$$

where K is a defect-concentration-dependent constant and, from the data in Fig. 2, $\alpha = \frac{1}{2}$. Indeed, we expect this behavior versus sample size to apply to superconducting materials with naturally occurring defects.

In summary we have studied the effect of defects in a

resistively shunted Josephson-junction array numerically in the context of breakdown phenomena at zero temperature and zero magnetic field. We have found that a single defect serves as a nucleation center for the vortices whose motions give rise to the dissipation of the system. The scaling relation between the critical current i_c and the defect size A is similar to that of the random-resistor problem for a long defect and hence the critical current is predicted to behave similarly to the breakdown threshold for linear electrical and mechanical breakdown problems. Although we have only studied arrays with single defects we expect the result to have implications for arrays with finite concentrations of random defects.

We are grateful to David Stroud for introducing us to the method of numerically solving the nonlinear differential equations used here and to Michael J. Stephen for stimulating discussions and helpful suggestions. We would also like to thank Philip M. Duxbury, William L. Mclean, T. Venkatesan, and G. Zimanyi for useful conversations. The support of the National Science Foundation through the John von Neumann Supercomputer Center is also gratefully acknowledged.

¹L. de Arcangelis, S. Redner, and H. J. Hermann, *J. Phys. (Paris) Lett.* **46**, L585 (1985).

²P. M. Duxbury, P. D. Beale, and P. L. Leath, *Phys. Rev. Lett.* **57**, 1052 (1986); P. M. Duxbury, P. L. Leath, and P. D. Beale, *Phys. Rev. B* **36**, 367 (1987).

³M. Sahimi and J. D. Goddard, *Phys. Rev. B* **33**, 7848 (1986); P. D. Beale and D. J. Srolovitz, *Phys. Rev. B* **37**, 5500 (1988).

⁴P. L. Leath and W. Tang, *Phys. Rev. B* **39**, 6485 (1989).

⁵J. S. Chung, K. H. Lee, and D. Stroud, *Phys. Rev. B* (to be published).

⁶S. R. Shenoy, *J. Phys. C* **18**, 5163 (1985); K. K. Mon and S. Teitel, *Phys. Rev. Lett.* **62**, 673 (1988).

⁷Ch. Leemann, Ph. Lerch, B. A. Racine, and P. Martinoli, *Phys. Rev. Lett.* **56**, 1291 (1986); R. K. Brown and J. C. Garland, *Phys. Rev. B* **33**, 7827 (1986); B. J. van Wees, H. S. J. van der Zant, and J. E. Mooij, *ibid.* **35**, 7291 (1987); M. G. Forrester, H. J. Lee, M. Tinkham, and C. J. Lobb, *ibid.* **37**, 5966 (1988).

⁸K. K. Likharev, *Rev. Mod. Phys.* **51**, 101 (1979).

⁹B. D. Josephson, *Phys. Rev. Lett.* **1**, 251 (1962); *Adv. Phys.* **14**, 419 (1965).

¹⁰The one exception is that when random initial conditions are used the numerical simulations show that a nonuniform mixture of superconducting and normal current distribution in the vertical direction seems to persist.

¹¹D. E. McCumber, *J. Appl. Phys.* **39**, 3113 (1968); W. C. Stewart, *Appl. Phys. Lett.* **12**, 277 (1968).

¹²Y. B. Kim and M. J. Stephen, in *Superconductivity*, edited by R. D. Parks (Marcel Dekker, New York, 1969), Vol. 2.